Building and Environment 196 (2021) 107801

Contents lists available at ScienceDirect

Building and Environment

journal homepage: http://www.elsevier.com/locate/buildenv

Simulation-assisted data-driven method for glare control with automated shading systems in office buildings

Jiarong Xie *, Azadeh Omidfar Sawyer

School of Architecture, Carnegie Mellon University, Pittsburgh, PA, USA

ARTICLE INFO

Keywords:
Visual comfort
Data-driven method
Glare-based shading control
Model-based control

ABSTRACT

An automated shading system is expected to effectively prevent visual discomfort associated with glare while providing adequate daylight penetration. However, the concept of visual comfort has not been well integrated into existing commercial shading systems, leaving potential for visual discomfort and resulting in occupants' dissatisfaction. Meanwhile, advanced methods in the academic literature are not always suitable for industrial applications due to problems associated with intensive real-time computation or privacy concerns. This research aims to address this gap by developing a simulation-assisted data-driven method for glare control with automated shades. The proposed strategy utilizes data from pre-simulated daylight analyses to develop glare predictive models using machine learning algorithms. With real-time solar irradiance measurements and the sun position as the input variables to feed the predictive models, the control algorithm can predict the glare condition and set the shades to an appropriate position that maximizes daylight ingress without causing glare. The presented method was verified using climate-based simulation to adjust the slat angle of automated venetian blinds in an office building. Its performance was compared to that of the conventional cut-off angle control for glare elimination, lighting use savings, and view access. The results showed that the proposed strategy was able to prevent 86.5%–96.9% of the glare and potentially reduce lighting energy use by 80.8% while the cut-off control only resulted in 28.9% glare elimination and 67.6% lighting energy savings. The presented method also allowed for unobstructed view more frequently, outperforming the cut-off angle control in all the examined categories.

1. Introduction

Access to daylight has been shown to have significant benefits for office workers' health, productivity, well-being, and satisfaction [1,2]. In addition to health benefits, making use of daylight (daylight harvesting) can also reduce building electric lighting use and the overall energy consumption. However, excessive and uncontrolled daylight from windows can cause glare, thermal discomfort, and increased building energy consumption. A balance between the benefits and drawbacks of daylight ingress is required to create a more satisfying, productive, and sustainable office environment. This balance can be achieved by using effective automated shading systems.

In 2019, Katsifaraki suggested that the function of automated shading control systems can be organized into three main categories [3]: 1) achieving visual comfort by providing sufficient daylight and view access without causing glare; 2) achieving thermal comfort by rejecting excessive solar penetration that could lead to overheating; 3) reducing building energy consumption by utilizing sunlight to decrease electric lighting use and heating energy demand. As discussed by Wymelenberg [4], the potential of daylight utilization to save energy must be provided in a manner that is acceptable to occupants, indicating the importance of prioritizing occupants' comfort for fenestration control. Meanwhile, field studies have reported that minimizing glare and visual discomfort is the major factor driving occupants to close blinds [5], further suggesting that a "glare-free" environment should take priority over other factors such as thermal comfort and energy saving when designing automated shading control strategies in office buildings. Accordingly, higher priority has been given to daylight and glare among existing studies on dynamic shading control as expressed in a most recent review paper [6].

Discomfort glare can be caused by excess brightness of the scene or high luminance contrast. Glare indices, such as the Daylight Glare Index (DGI) [7] and Daylight Glare Probability (DGP) [8], have been proposed to estimate the likelihood of an observer experiencing visual discomfort. In a 2019 study, Wienold et al. evaluated the performance and robustness of 22 established glare indices using experimental datasets of

* Corresponding author. Room 415, Margaret Morrison Carnegie Hall, Carnegie Mellon University, Pittsburgh, PA, USA.
E-mail address: jiarongx@andrew.cmu.edu (J. Xie).

https://doi.org/10.1016/j.buildenv.2021.107801
Received 8 December 2020; Received in revised form 10 March 2021; Accepted 12 March 2021
Available online 17 March 2021

daylight-dominant workplaces in different locations [9]. They found that DGP outperformed the other indices in describing the glare scale and distinguishing between disturbing and non-disturbing scenes. As summarized in two review papers, DGP is one of the most widely used metrics for solar radiation control, glare evaluation, and indoor visual comfort assessment [6,10]. According to Wienold and Christoffersen [8], DGP is a function of the vertical eye illuminance as well as of glare source luminance:

$$DGP = 5.87 \times 10^{-5} \times E_v + 9.18 \times 10^{-2} \log\left(1 + \sum_{i=1}^{n} \frac{L_i^2 \times \omega_i}{E_v^{1.87} \times P_i^2}\right) + 0.16 \quad (1)$$

where E_v is eye-level vertical illuminance (lux), ω_i is the solid angle of the glare source (sr), L_i is the luminance level of the glare source (cd/m^2), and P_i is the Guth position index expressing the occupants' sensitivity within their field of view. A simplified DGP (DGPs) was later proposed which omits the influence of individual glare sources and greatly simplifies the calculation of glare perception [11]. However, it can only be applied if no direct sun or specular reflection from the shades is within occupants' field of view [12].

As reviewed by Katsifaraki [3], most existing commercial shading systems implement relatively simple control strategies, such as activating shades based on time, the position of the sun, and work plane illuminance. The concept of discomfort glare is not well integrated into the control strategies of these systems, potentially compromising their performance in satisfying occupants' requirements for visual comfort. For instance, a previous study reported that a typical automated venetian blind system that was controlled based on the vertical illuminance led to 45% of the control actions being overridden by occupants [13], indicating its shortcoming to meet occupants' expectations and satisfaction. There have been several studies on dynamic shading control that capture real-time glare using a High Dynamic Range (HDR) vision sensor [14,15] or camera [16]. However, it is important to note here that taking pictures of the workplace could cause privacy concerns among occupants, especially in an open-plan office. Another method proposed by researchers is to employ real-time daylight simulation to obtain glare indices [17,18]. This method could be computationally intensive and may lead to a slow response of the control system, and potentially overload the controller of the Building Automation System (BAS). Currently, there are limited daylight simulation tools that are fast and user-friendly enough to be integrated into the control system [19]. Therefore, the real-time daylight simulation may be "a significant limitation and obstacle for simulation assisted controls to become an industrial application" [19].

Many studies have proposed to use simple measures to replace glare indices to quantify discomfort glare [20–28]. These metrics can be categorized as illuminance- and luminance-based measures. Of the illuminance-based measures, horizontal illuminance has been recommended as an indicator of visual discomfort in the perimeter zones in offices in several studies [4,20,21,29]. However, a study by Konis [22] found that occupants sitting in the core zone of a side-lit office reported visual discomfort even with very low horizontal illuminance. He suggested that occupants' perception of visual discomfort may be context-specific, depending on their distance to the façade and the interior surface reflections. Another experimental study also reported that work plane illuminance and DGP were not well correlated [23]. Therefore, more studies are required to support the use of horizontal illuminance to quantify glare with the context specified. Numerous studies have investigated the correlation between vertical eye illuminance and perceived visual discomfort by occupants, suggesting it is a promising indicator of discomfort glare [4,23,24,30,31] Nevertheless, there is a large variation in the proposed thresholds of visual discomfort, ranging from 375 lux [24] to 3000 lux [31]. There is no consensus among researchers regarding what threshold should be used. Some newly proposed metrics like the cylindrical illuminance and vertical illuminance vector require more verification, especially experimental validation [25]. Another major limitation of all illuminance-based measures is that they are not adequate to represent contrast-based glare. Therefore, they are not suitable for places where contrast is dominant, such as those with large windows and specular monitor screens. Recommended luminance-based metrics include maximum luminance [24,32], luminance contrast ratio [22,31], and mean luminance [4], etc. They have similar limitations as glare indices when applied in dynamic shading control, i.e, physical measurements may cause privacy concerns and real-time simulation can be challenging. Wienold proposed the simulation-based metric-enhanced simplified DGP which separates the computation of the illuminance and luminance contrast of DGP and uses a simplified image to derive it [33]. However, the validation of this method indicates that it may not apply to scattering or re-directing façade designs. To summarize, these simple measures are not sufficient to fully replace glare indices given that each of them has specific limitations in glare quantification.

To overcome the drawbacks of existing methods and integrate visual comfort into automated shading systems in a practical manner, a promising solution would be a data-driven approach [19]. As indicated in a recent review paper, machine learning algorithms (MLAs) have been widely used in existing studies to predict indoor daylighting conditions [34]. It has gained much popularity in the building design community due to its capability to surrogate complex daylight simulations. However, only a few studies can be found which have explored the use of MLAs for dynamic shading control. Most studies on using MLAs to predict daylighting focused on the estimation of illuminance or daylight availability such as Spatial Daylight Autonomy (sDA) and Useful Daylight Illuminance (UDI). As indicated in a recent review study on MLAs to predict daylighting inside buildings by Ayoub [34], 53% of the 27 selected studies concentrated on the prediction of illuminance, and the other 40% on daylight availability metrics. Only two studies on predicting visual comfort were identified [35,36]. One suggested that DGP prediction with MLAs did not show a satisfying result [36]. This might be explained by the fact that glare is affected by additional factors (such as view directions), making its prediction more complex compared to illuminance or illuminance-based metrics. It should be noted that both studies applied a regression model to predict DGP, which could potentially compromise the model accuracy due to limited model inputs. As indicated by Ayoub [34], the classification and clustering method might be more appropriate for visual comfort prediction that entails classifying daylight conditions. More research is required to investigate the performance of predicting visual comfort using MLAs.

This study aims to propose a glare-based dynamic shading control strategy that is applicable in complex real-world settings, especially in open-plan offices. It investigated the feasibility of using machine learning (ML) classification models developed from pre-simulated data to predict glare in physical environments. Specifically, the models were trained with pre-simulated data from daylight modeling using Typical Meteorological Year (TMY) weather, with the position of the shades as a variable. With real-time measured input variables such as solar irradiance to feed the predictive models, the control algorithm set the shades to the position that maximized daylight ingress without causing glare. This application of the proposed strategy was demonstrated to control the venetian blinds in a simulated open-plan office. Its effectiveness in preventing glare while maximizing daylight and view access was validated with actual historical weather. Automated shading systems can be generally divided into open-loop and closed-loop control systems [37]. The presented control method in this study is an open-loop strategy. Jain and Garg reviewed open-loop control strategies for automated shading and integrated lighting control that utilize real-time daylight prediction and concluded that advanced open-loop control systems using calibrated simulations are more advantageous than closed-loop systems in reducing post-commissioning errors, easy monitoring, and predicting daylight more extensively [19]. They also stated that few studies have incorporated learning algorithms into the control process to replace

physical daylight modeling. This study is an exploration to address this gap.

2. Methodology

2.1. Overall workflow

The proposed shading control method aims to predict real-time discomfort glare using data-driven models developed from daylight simulations and control the shading devices accordingly. The workflow to achieve this goal can be divided into three phases: the pre-simulation phase, the ML model development phase, and the real-time control phase. In the pre-simulation phase, a daylight simulation program was required to generate the annual hourly glare profile for ML model training. In the predictive model training phase, individual models for different shading states were developed using the pre-simulated data. Several common ML classification models, such as Random Forest were used to predict visual comfort. The hyperparameters of each model were optimized to select the model that gave the highest prediction performance. In the real-time control phase, concurrent solar irradiance measured by a pyranometer on the rooftop was used to feed the ML models. At each time step, the shading control algorithm searched for the state of the shades that allowed for maximum daylight ingress without causing glare, and the system took that position as the control command. Fig. 1 illustrates the application of the workflow to operate multiple (groups of) shades facing different ordinal orientations, which is common in open-plan offices.

2.2. Machine learning classification algorithm

Three classification algorithms were used for glare prediction, including K-nearest neighbor (KNN) [38], Support Vector Machine (SVM) [39], and Random Forest (RF) [40]. These methods were selected for the following reasons: 1) they are simple and easy to implement; 2) prediction with these models is quick, which would not cause computation burden in the controller for real-life applications; 3) they are the most common and widely used classification algorithms in similar research studies.

2.2.1. K-nearest neighbor

KNN is one of the simplest machine learning methods that has been used since the early 1970s in statistical applications. It is a non-parametric approach that does not require assumptions about how the input variables are correlated to the output variable. The logic behind this method is that it searches for a group of k samples that are nearest to the unknown sample according to the distance between the known sample and the new sample. The class of the new sample is usually determined by the majority class of the k samples. Hence, k is the only tuning parameter that determines the predicting performance of this classifier.

2.2.2. Support Vector Machine

SVM is a machine learning algorithm for two-group classification problems. Fig. 2 illustrates an example of SVM classification with a linear separation hyperplane. The main objective of this method is to find a separation hyperplane that gives the greatest distance between two classes using support vectors. It should be noted that by mapping the input variables into a higher dimensional feature space, the hyperplane can be nonlinear as well. Accordingly, the SVM classifier can have a nonlinear kernel. In this study, a common radial basis function (RBF) kernel was used. The regularization parameter (C) was specified in this study.

2.2.3. Random Forest

Compared with KNN and SVM, RF is an ensemble method that grows many decision trees in parallel with bootstrapping. Each decision tree gives a classification, which is called the "votes" for that class by the tree. The forest chooses the classification having the most votes (over all the trees in the forest). Two parameters that greatly affect the performance of an RF model were specified in this study, including the number of trees (N) and the maximum depth of each tree (d). By limiting the maximum depth of each tree, RF builds smaller trees to prevent overfitting. Hence, an RF classifier usually outperforms a decision tree classifier.

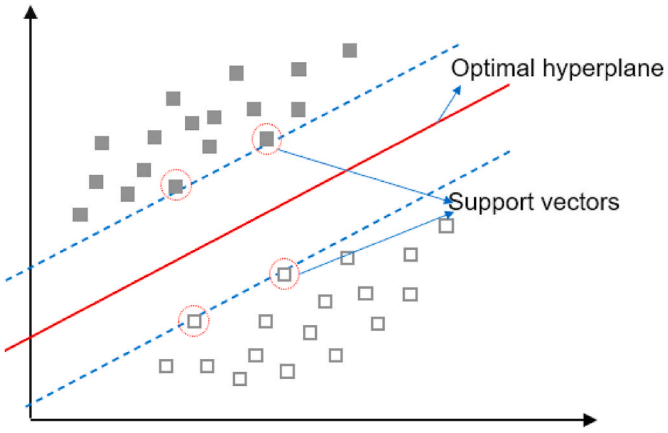

Fig. 2. An example of SVM classification.

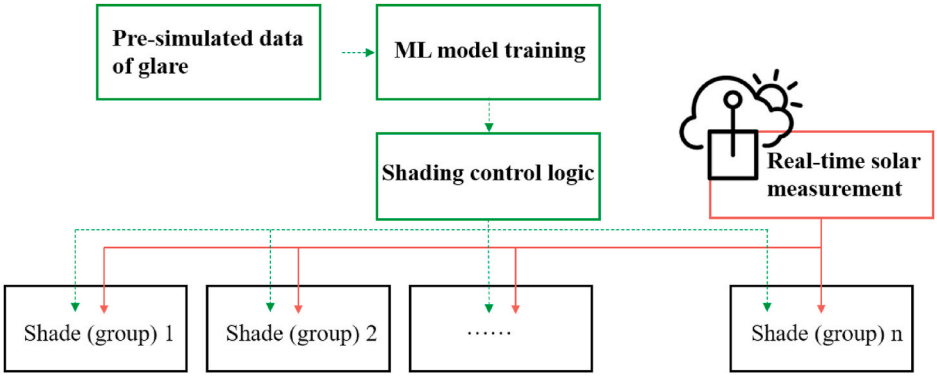

Fig. 1. The flowchart for the overall workflow to operate multiple shades. (For interpretation of the references to colour in this figure legend, the reader is referred to the Web version of this article.)

2.3. Development of a case study

2.3.1. Description of the case building

The Intelligent Workplace (IW), an existing open-plan office at Carnegie Mellon University, was used to validate the proposed control strategy. It occupies the top floor of the Margret Morrison Hall that is located in Pittsburgh, Pennsylvania, USA (latitude 40.4 N, longitude 80 W). The office is highly glazed, with a window-to-wall ratio that is close to 70%. It is equipped with internal automatic venetian blinds that were used to test the presented control strategy. The blinds can be adjusted by changing the tilt angle of the slats. The slats are flat lamellae with a width of 0.05 m that are spaced 0.05 m apart. They are purely specular metal materials with a specularity of 0.8. The venetian blind system allows the tilt angle to rotate from 0° (fully open) to 90° (fully closed) as shown in Fig. 4, with an interval of 15°. One workstation facing the east (marked as the blue rectangle in Fig. 3) was selected to demonstrate the application of the control method. As indicated in Fig. 3, the green dot represents the occupant's sitting position (1.2 m above the finish floor) and the red dot is the selected reference point to quantify the illuminance on the work plan (0.8 m above the finish floor).

2.3.2. Glare simulation

The software Rhinoceros was used to construct the geometry of the simulation model. Rhinoceros (Rhino) is a stand-alone, commercial NURBS-based 3D modeling tool, developed by Robert McNeel and Associates [41]. DIVA for Grasshopper was used to perform point-in-time glare simulation to obtain hourly DGP. DIVA is an environmental analysis plugin in both Rhino and Grasshopper. The DIVA environment supports a series of performance evaluations by using validated tools including Radiance and Daysim [42]. Perez All-Weather Sky Model was applied for the simulation to better represent the actual

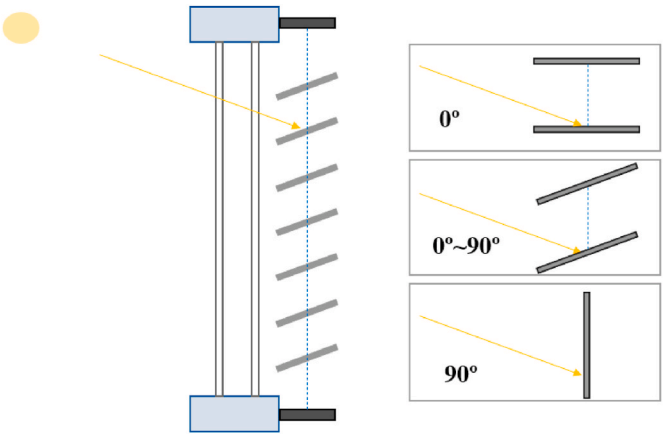

Fig. 4. Blind slat angle control range.

(a)

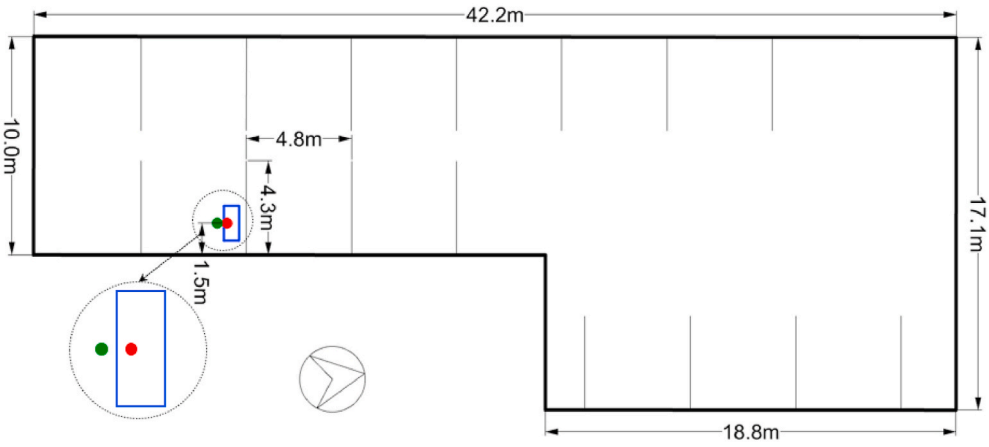

(b)

Fig. 3. The Intelligent Workplace (a) and its floor plan (b) with the selected workstation.

climatic situations and cover all possible sky conditions. The properties of materials used in the simulation are listed in Table 1 and the Radiance parameters for HDR rendering are summarized in Table 2. Both specularity and roughness for the plastic materials are 0. The PC monitor was modeled as glow material with luminance of 250 cd/m^2. A Grasshopper workflow was created to automatically run the simulation for the entire year and record the simulation results. The hourly simulation was conducted during occupied hours, resulting in a total of 4015 simulations in a year. The annual simulation was repeated with blinds at varied slat angles from 0° to 90°, with an interval of 15°. The simulation data with TMY weather were used for ML model training and the data with the year 2018 weather were used to verify the control strategy. The solar irradiance data for the year 2018 were obtained from the National Solar Radiation Data Base (NSRDB) created by the National Renewable Energy Laboratory (NREL). The NSRDB is a publicly open dataset that consists of solar radiation and meteorological data over the United States as well as regions of the surrounding countries. It provides half-hourly and hourly solar irradiance data at a 4-km horizontal resolution from 1998 to 2019. The data were computed from multi-channel measurements from geostationary satellites using the NREL Physical Solar Model and have been validated using ground-based measurements [43–45]. The most recent study shows that the mean percentage bias was −2.6 to 4.0% for Global Horizontal Irradiance (GHI) and −2.7 to 15.9% for Direct Normal Irradiance (DNI) on an hourly basis, depending on the location [43]. Given that the percentage bias for the GHI at the surface sites is around 5% [45], the hourly NSRDB data can be used as an acceptable substitute to station observations that might not be available. It is recommended that the dataset be used for developing TMY data for building design and comparison of solar system performance [45]. The hourly solar irradiance data used in this study were downloaded using the NSRDB Viewer (https://nsrdb.nrel.gov/nsrdb-viewer).

2.3.3. ML model development

Fig. 5 illustrates the ML process of developing glare predictive models. It follows a standard machine learning pipeline, including data processing, model selection, model training, and testing. Separate models for each of the selected slat angles were trained. The process was conducted using the machine learning module for Python (https://www.kite.com/python/docs/sklearn).

- **Data processing - SMOTE for imbalanced dataset**

According to Wienold and Christoffersen [8], glare is classified as imperceptible, perceptible, disturbing, and intolerable glare. They proposed the thresholds and later revised them in a cross-validation study [9]. The validation data were collected within the human subject from Argentina, Denmark, Germany, Japan, Israel, and the US. The updated ranges are shown in Table 3. A threshold of 0.35 for DGP indicating perceptible glare was used to label the outcome variable as “Glare” or “No glare”. This value and slightly smaller values (such as 0.32 [16] and 0.3 [14]) have been commonly used in existing studies on glare-based shading control [14,16–18,46]. As a result, the obtained dataset was imbalanced, with more glary cases than non-glary cases. The dataset became more imbalanced as the slat angle of the blinds increased. ML models trained using such a dataset would give a poor performance on the minority class, i.e., cases with glare. To address this problem, the technique of oversampling the minority class was applied. Specifically, the simplest oversampling approach that duplicates examples in the minority class was used. Although these examples did not add any new information to the model, new examples can be synthesized from the existing examples to balance the class distribution. This is a type of data augmentation for the minority class that is referred to as the Synthetic Minority Oversampling Technique or SMOTE for short. The ratio of the number of samples in the minority class over the number of samples in the majority class after resampling can be defined. In this study, a value of 1 was used. Fig. 6 visualizes how the number of data points of the minor class were increased using the SMOTE.

Table 1
Material descriptions for the daylight simulation model.

Opaque Material	Material Type	Red Reflectance	Green Reflectance	Blue Reflectance
Ceiling	Plastic	0.7	0.7	0.7
Wall	Plastic	0.7	0.7	0.7
Floor	Plastic	0.2	0.2	0.2
Blinds	Metal	0.8	0.8	0.8
Desk	Plastic	0.5	0.5	0.5
Partition	Plastic	0.5	0.5	0.5
Glazing Material		Red Transmissivity	Green Transmissivity	Blue Transmissivity
Window glaze	Glass	0.87	0.87	0.87

Table 2
Radiance parameters for the HDR renderings for DGP simulation.

Parameter	Value
Direct jitter (-dj)	0
Direct sampling (-ds)	0.5
Direct threshold (-dt)	0.5
Direct certainty (-dc)	0.25
Direct relays (-dr)	0
Direct pretest (-dp)	64
Specular threshold (-st)	0.85
Ambient bounce (-ab)	2
Ambient accuracy (-aa)	0.25
Ambient resolution (-ar)	16
Ambient divisions (-ad)	512
Ambient super-sample (-as)	128
Ray reflection limit (-lr)	4
Ray weight limit (-lw)	0.05

- **Selection of model input variables**

In this study, the sitting position and the view direction of the occupant were predefined. For the given workstation, factors that can have a significant impact on the glare condition include the intensity of solar irradiance and the position of the sun. At a specific time, the position of the sun can be described by the azimuth angle and the altitude angle, while the solar condition can be described with Diffuse Horizontal Irradiance (DHI) and DNI. These four variables are widely used in existing studies predicting daylight with MLAs [34], and they are also easy to obtain for real-time shading control. Therefore, they were selected as the model input.

- **Model evaluation metrics**

The confusion matrix, also known as the error matrix, is widely used to describe the performance of a classification model (or a classifier). The confusion matrix for the binary classifier in this research is shown in Table 4. In this study, the consequence of False Negative, meaning the model fails to predict the occurrence of actual glare, is more serious than False Positive. Thus, the recall score, a measure of the correctly identified positive cases from all the actual positive cases, was used as the model evaluation metric. Recall score can be calculated using Equation (2).

$$Recall = \frac{\text{True Positive}}{\text{True Positive} + \text{False Negative}} \quad (2)$$

- **Hyperparameter tuning**

In machine learning, a model hyperparameter is a pre-defined

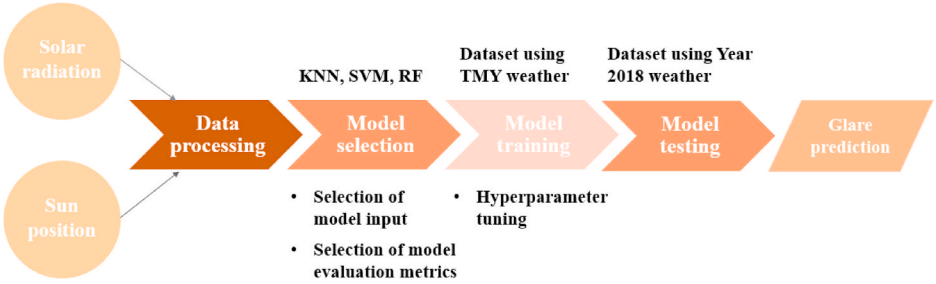

Fig. 5. ML process for developing the glare predictive models.

Table 3
DGP and glare condition.

Daylight Glare Probability	Glare condition
DGP <0.35	Imperceptible glare
0.35 ≤ DGP ≤0.38	Perceptible glare
0.38 < DGP ≤0.45	Disturbing glare
>0.45	Intolerable glare

configuration to control the learning process. It is external to the model and cannot be estimated from the traning data. The purpose of hyperparameter tuning is to optimize a single target evaluation metric. In this study, the hyperparameters of each ML model were optimized with recall score as the target. A grid search along a few selected parameters of each classifier was conducted. Where additional parameters beyond the ones considered exist, they were kept at the default values offered by their respective implementations. The hyperparameters which gave the highest recall score on the validation dataset were selected. The tuning process was implemented using cross-validation, a procedure to evaluate the performance of ML models. It has a single parameter called k that refers to the number of subgroups (folds) that a given dataset is to be split into. Of the k subsamples, k-1 groups are used as the training data, and the rest single subsample is retained as the validation data for testing the model. This process is then repeated k times, with each of the k subsamples used exactly once as the validation data. The k results from each process can then be averaged and used to evaluate the performance of the model. In this study, the common 10-Fold Cross-Validation was used. The examined hyperparameters for each model as well as their searching range are listed in Table 5.

2.3.4. Implementation of the proposed control framework using simulation

The overall workflow of the proposed control logic is shown in Fig. 7. From the simulation, the minimal slat angle that can be used to fully prevent glare at any time during the occupied hours is determined, which is the maximum of the selected slat angles for real-time blind control. With solar irradiance measurements (DHI and DNI) and calculated sun position (azimuth and altitude angle), the control logic aims to find the smallest slat angle that can eliminate glare and set it as the tilt angle at the current timestep. Specifically, the logic first predicts if there is glare with a slat angle of 0°. If there is no glare, the slat angle is set as 0°. Otherwise, the control logic examines if there is glare with a slat angle of the second smallest angle and repeats the previous decision-making process.

3. Result

3.1. Comparisons between the TMY and historical weather data

The historical year 2018 weather was compared to the TMY weather within the occupied time from different perspectives. Fig. 8 and Table 6 provide the statistics of the two weather datasets. Generally, the actual weather had higher DNI and lower GHI and DHI compared to the TMY weather. Notably, the standard deviation of DHI for the actual weather was much smaller than that of the TMY weather. The sky condition was

Table 4
Confusion matrix for the binary classifier in this study.

	Predicted		
Actual		Glare = Yes	Glare = No
	Glare = Yes	True Positive (TP)	False Negative (FN)
	Glare = No	False Positive (FP)	True Negative (TN)

Table 5
The examined hyperparameters and the range of each model.

Model	KNN	SVM	RF
Hyperparameters and their examined range	Number of neighbors K ∈ [10,47] with an interval of 1	Regularization parameter C ∈ [1, 20] with an interval of 1	The number of trees N and the maximum depth of each tree d, N ∈ [1,20] with an interval of 1, d ∈ [1,6] with an interval of 1

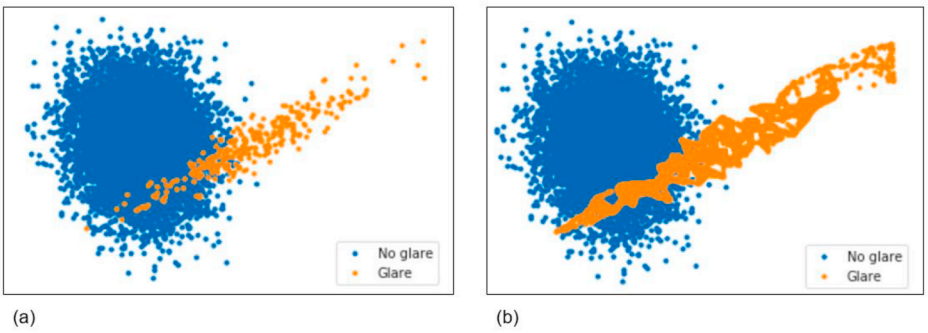

Fig. 6. Visualization of the training dataset: (a) original dataset; (b) the dataset after applying SMOTE.

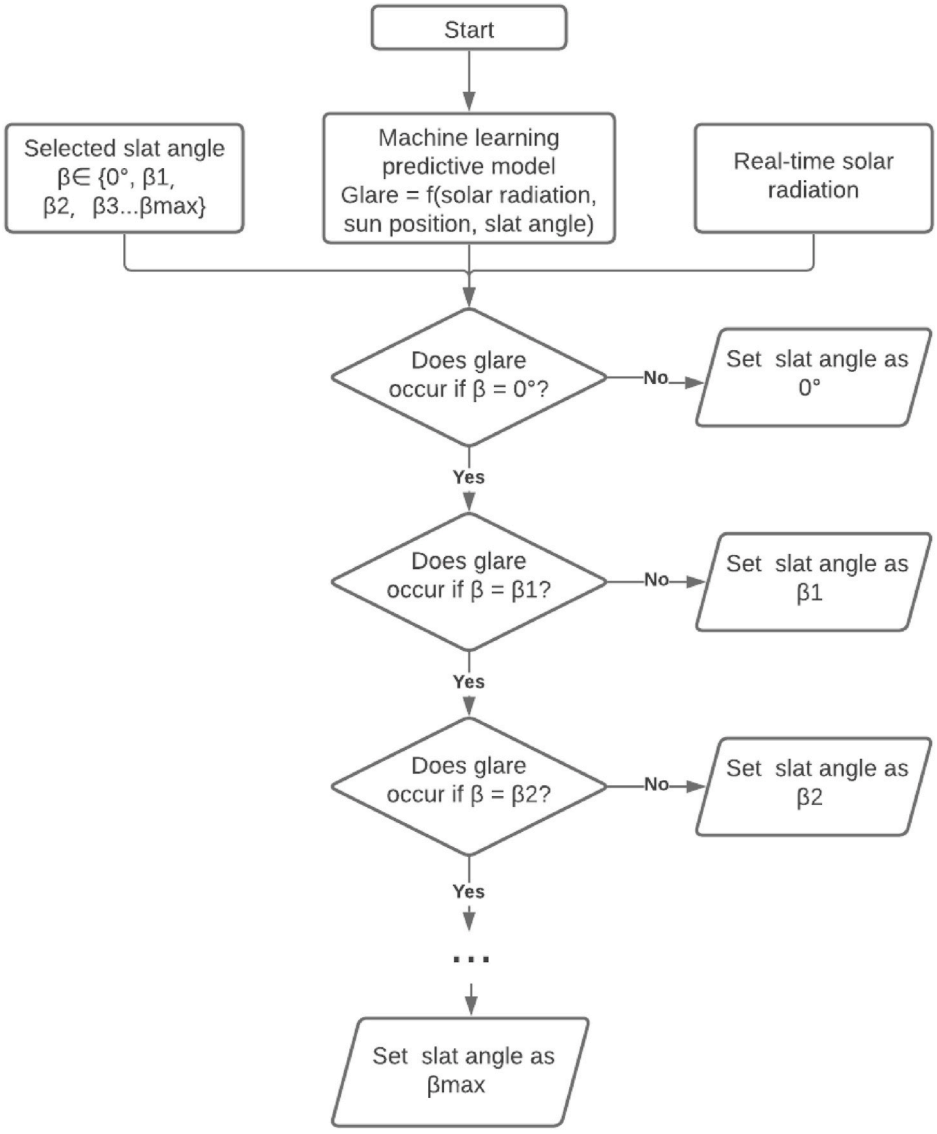

Fig. 7. Overall workflow of the proposed control logic.

further analyzed to investigate the variation between the two weather. It was determined based on a model proposed by Fakra et al. [48]:

$$SR = \frac{\mathrm{DHI}}{\mathrm{GHI}} \tag{3}$$

where SR is the Sky Ratio. Three sky condition categories were defined according to SR as proposed by Motamed et al. [49], which is listed in Table 7. As illustrated in Fig. 9, the 2018 weather had slightly fewer partially cloudy days and more clear and overcast days compared to the TMY weather.

3.2. Annual glare analysis with the training dataset

A total of 3820 data points for each annual simulation were obtained. Table 8 lists the number of hours with and without glare as well as their ratio at different slat angles. The original dataset was substantially imbalanced, with most of the hours devoid of glare. The imbalance was more significant with the increase of the slat angle. This indicates the necessity of applying the SMOTE technique to address this problem to improve the performance of the predictive models. Additionally, it is important to highlight that there was no glare case in the training dataset when the slat angle was 45° and above. Hence, only 0°, 15°, 30°, and 45° were selected for the control of the blinds, and three individual models were trained for glare prediction (for 0°, 15°, and 30°).

3.3. Performance of different ML models

Fig. 10 illustrates the recall score of different models with their tuned hyperparameters. As shown in the figure, all three models had a high recall score (0.92–0.98) with a slat tilt angle of 0°. The recall score for the model with a slat angle of 15° was also satisfying for the SVM and RF models. The performance of the KNN model was lower but still acceptable. As the slat angle increased to 30°, both KNN and RF methods had a significantly lower recall score than the 0° and 15° model while the SVM maintained a good performance. Overall, the SVM algorithm seemed to exhibit a robust and stable prediction ability for the glare cases despite the imbalance of the original dataset before applying SMOTE. In contrast, the performance of the other two algorithms was more sensitive to the quality of the original training dataset, i.e, how imbalanced it was, especially the KNN algorithm.

3.4. Evaluation of the proposed control strategy

The proposed control algorithm was compared with the conventional

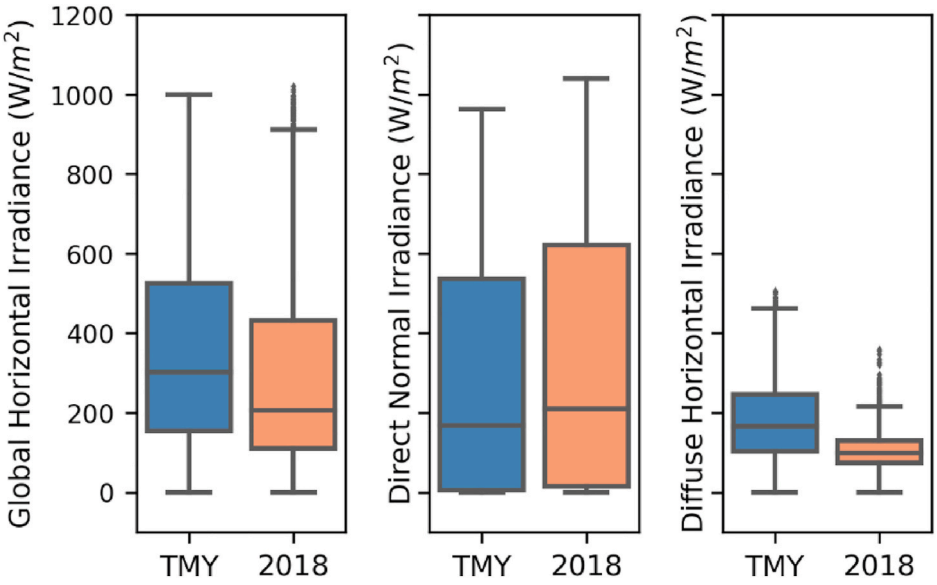

Fig. 8. Boxplots of the solar irradiance of the TMY weather and 2018 weather.

Table 6
Mean and standard error of the two weather datasets.

	GHI (W/m^2)		DNI (W/m^2)		DHI (W/m^2)	
	TMY	2018	TMY	2018	TMY	2018
Mean	354.7	294.5	283.2	322.8	180.4	103.8
Standard deviation	244.2	236.3	289.3	323.1	103.6	46.1

Table 7
Sky condition category and SR [49].

Sky Ratio	Sky Condition
SR $<$ 0.3	Clear
0.3 $\leq$ SR $<$ 0.8	Partially cloudy
SR $\geq$ 0.8	Overcast

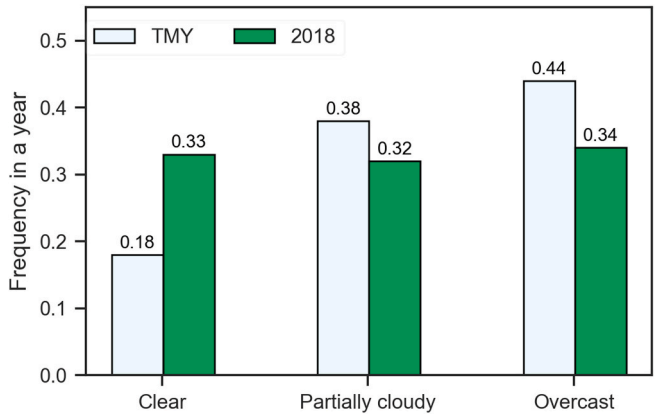

Fig. 9. The sky condition distribution of the two weather.

cut-off angle control, in relation to glare prevention, potential in reducing lighting energy use, and view access. Cut-off control tilts the blind slats to the angle beyond which no direct solar radiation can penetrate. The cut-off angle can be calculated according to the solar profile angle as proposed by Karlsen et al. [30].

Table 8
Number of hours with glare and without glare with the TMY weather.

Blind slat angle	Glare	No Glare	Glare: No Glare before using SMOTE	Glare: No Glare after using SMOTE
0°	290	3530	1:12	1:1
15°	44	3776	1:86	1:1
30°	10	3810	1:381	1:1
45°	0	3820	–	–
60°	0	3820	–	–
75°	0	3820	–	–
90°	0	3820	–	–

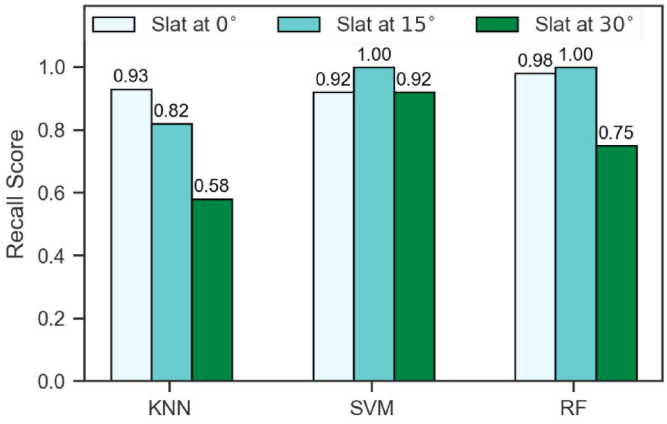

Fig. 10. The recall score of different models with the tuned hyperparameters.

$$\beta_{cut-off} = sin^{-1}\left(\cos(\Omega)\cdot\frac{s}{w}\right) - d \quad (4)$$

$$\Omega = tan^{-1}(tan\alpha / cos\gamma) \quad (5)$$

where $\beta_{cut\text{-}off}$ is the cut-off angle (rad), Ω is the solar profile angle (rad), s is the spacing between the blind slats (m), w is the width of the slats (m), α is the solar altitude angle (rad), and γ is the solar surface azimuth angle (rad).

3.4.1. Annual glare analysis

In this study, "on-state-hit" and "off-state-missed" were defined to evaluate the performance of the shading control strategy in preventing glare. "On-state-hit" refers to cases where glare was detected, and the automated shading system activated correctly to eliminate glare. "Off-state-missed" refers to cases when glare occurred and the automated shading system failed to activate or it activated but failed to prevent glare. Table 9 shows an example for each of these two scenarios on April 10th with the SVM classifier. At 9 a.m., the ML model correctly predicted the occurrence of glare with the blind slat at 0°. Then the control algorithm proceeded to check the condition if the blind was rotated to 15°. The SVM model accurately predicted there was no glare and the control algorithm set this angle as the control command. As a result, glare was successfully prevented. In contrast, at 10 a.m., the SVM classifier failed to predict glare incidents with the blind slat at 0°. Accordingly, the algorithm then set 0° as the command. In this case, glare was not eliminated.

The percent of "on-state-hit" and "off-state-missed" with cut-off control and the proposed control based on different ML algorithms is illustrated in Fig. 11. It is important to highlight that the cut-off angle control performed poorly in eliminating glare, with an "on-state-hit" percentage of 28.9%. The proposed control strategy significantly outperformed the cut-off control despite the ML algorithm used. In particular, 96.9% of the glare was eliminated if RF-based predictive models were used. The SVM- and KNN-based control algorithm also had a satisfying performance, with an "on-state-hit" of 91.7% and 86.5%, respectively. The result illustrates the excellent capability of the proposed control strategy in preventing glare.

3.4.2. The potential in reducing lighting energy use

The potential of the proposed strategy and the cut-off shading control in lighting energy savings was estimated based on the reduction of the number of hours that require artificial lighting use. For each of the strategies, it was assumed that electric lights are switched off when the illuminance on the work plane is above 500 lux. The default setting is an on/off lighting control that is toggled based on office hours, i.e. all lighting devices are switched on during office hours (8 a.m.–6 p.m.). As indicated in Table 10, lighting energy saving rates of 80.8% can be achieved with the proposed shading control strategy, despite the ML algorithm used. The difference in lighting energy use reduction due to the classification algorithm was negligible. The cut-off control strategy also had a substantial potential in reducing lighting energy use, yet notably lower than the proposed control method.

3.4.3. View access

The distribution of annual blind slat tilt angle with the proposed and cut-off shading control strategy is illustrated in Fig. 12. The cut-off angle was rounded to the nearest multiple of 15° and the negative angle was replaced with 0°. With cut-off angel control, the blind was kept fully open for 60% of the occupied time. This percentage was 86%–90% with the proposed control strategy, suggesting a significant improvement in view access for the occupants, which could improve their satisfaction with the proposed control strategy in real-life applications.

3.5. Validating the proposed method with a different climate

As discussed in Section 2.3.3, the performance of the ML predictive model depends on the quality of the training dataset. A more balanced dataset would result in a model with a higher recall score, further improving the capability of the proposed shading control strategy to avoid glare. In this study, the dataset was generated from daylight simulation with a cloudy climate, resulting in fewer samples with glare than without glare. Thus, it is hypothesized that the proposed control algorithm will have better performance if validated with a sunny climate. To test this hypothesis, we selected Phoenix, Arizona for further verification. All the building and model settings were kept the same for the new climate.

As shown in Fig. 13, the performance of the proposed control algorithm improved when it was validated with a sunny climate. Specifically, the "on-state-hit" percent increased to 93.5% for KNN model-based control, 95.6% for SVM, and 98.6% for RF. The result confirmed our hypothesis, suggesting that the proposed control strategy is more advantageous if applied in locations with a sunny climate.

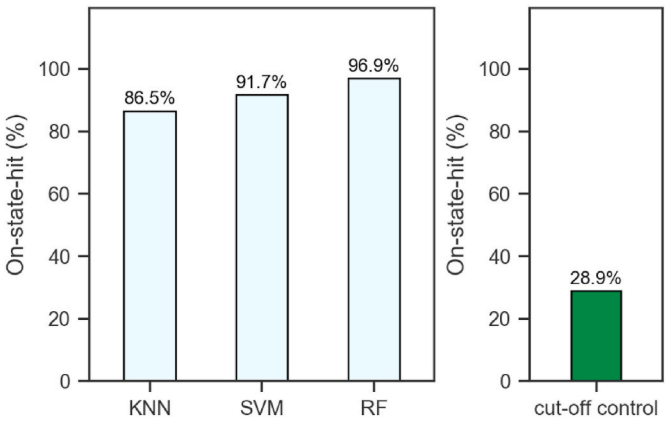

Fig. 11. The percentage of "on-state-hit".

Table 10
The potential in lighting energy use reduction.

	ML algorithm	Lighting energy use reduction
The proposed control strategy	KNN	80.8%
	SVM	80.8%
	RF	80.8%
Cut-off control	–	67.6%

4. Discussion

This study proposed a data-driven method to integrate the concept of visual comfort into the control of automated shading systems, seeking a feasible glare control solution for real-life applications. The presented strategy replaced intensive real-time daylight simulation in conventional model-based control with simple ML predictive models developed from pre-simulated data. Meanwhile, it eliminates the use of indoor physical sensors that could cause various concerns such as privacy, sensor placement, and aesthetics. The control strategy was validated in an existing office building using simulation with actual historical weather data, illustrating the capability of ML algorithms in preventing up to 96.9% of the glare, thus, greatly outperforming the conventional cut-off angle control. It also improved view access and potential in

Table 9
An example of "On-state-hit" and "Off-state-missed" with the SVM algorithm (1 - with glare; 0 - without glare).

Time	Glare with the slat at 0°		Glare with the slat at 15°		Glare with the slat at 30°		Control outcome
	Predicted	True	Predicted	True	Predicted	True	
Apr 10th, 9 a.m.	1	1	0	0	0	0	"On-state-hit"
Apr 10th, 10 a.m.	0	1	0	0	0	0	"Off-state-missed"

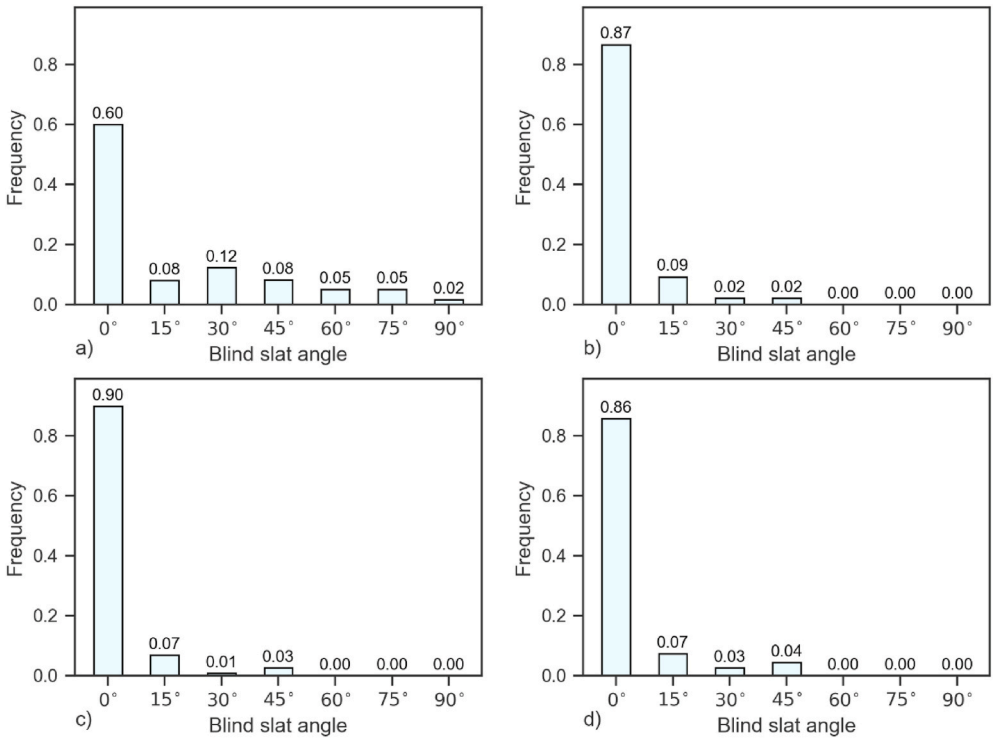

Fig. 12. The distribution of blind slat tilt angle: a) cut-off control; b) KNN model-based control c) SVM model-based control d) RF model-based control.

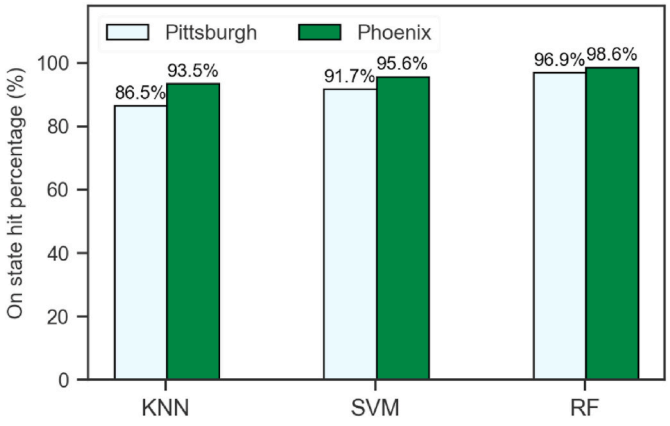

Fig. 13. The percentage of "on-state-hit" with the proposed control strategy with a sunny climate and a cloudy climate.

reducing lighting energy use compared to the cut-off control. The result suggests that the presented control strategy is a promising solution to balance the benefits and drawbacks of daylight ingress in real-life office environments.

It is worth noting that there have been some recent studies on daylighting control using a simplified predictive model [46,50,47]. These methods are also capable of minimizing the use of indoor sensors and eliminating real-time daylight simulation. The main idea is to use pre-defined correlations between the control variable and another physical measure that is easier to obtain. For instance, work plane illuminance can be controlled within 500–2000 lux according to the real-time measurement or simulation of exterior window illuminance. It should be noted that the main problem with these methods is that the pre-obtained correlation varies with the data used to derive it. The pre-derived equation might not work when it is implemented in the control system, due to the variation in the weather condition. Furthermore, it also varies with the day of the year and time of the day, as well as the states of the shading devices. Hence, one or several fixed equations might not be representative or sufficient to describe the underlying correlation. Thereby, the performance of the control strategy that depends on the pre-determined equations can be compromised. On the contrary, the control method proposed in this study takes advantage of the learning and predictive feature of MLAs to respond to new data to achieve better predictive capabilities. As revealed by the result, the model trained from simulation data with TMY weather had a good performance when it was used to predict glare using actual weather.

Under the assumption that the daylight simulation model is well-calibrated, this research showed that ML predictive models developed from pre-simulated data can be used for real-time shading control. In practice, the system will also be commissioned before it is installed, to further ensure the accuracy of the predictive model. Thereby, physical measurements to collect data for developing the ML models can be eliminated. The ML models used in this study are simple, allowing for very fast computation. Thus, it is possible to account for multiple view directions for more accurate glare evaluation and customize the shading control strategy in private offices. Additionally, the proposed method can be used to control shading groups facing different orientations in open-plan offices. It is also applicable to control other types of shades.

Despite the strengths, several challenges need to be addressed in future studies. The primary challenge is how to minimize the dataset required to develop a reliable predictive model. This is especially important if the proposed method is used to control multiple shades in open-plan offices or multiple view directions are considered for effective glare control. Sensitivity analysis in training dataset size and model ML model performance should be conducted to answer this question. It is further suggested that an analysis of the spatial distribution of glare should be conducted to apply this method to control multiple shades in the open-plan office. Advances in daylight simulation tools that allow for fast and concurrent glare computation at multiple sitting positions with multiple view directions will be of great use for such analysis. The newly developed tool ClimateStudio by Solemma LLC is an excellent example of these advanced tools (https://www.solemma.com/ClimateStudio.html). It performs daylight simulation using Radiance as the

engine. However, it implements Radiance in a progressive path tracing mode that traces few paths at a time and updates the result as the simulation progresses instead of tracing all possible light paths before computing a result. Combined with the use of GPU to handle mathematical operations, it allows for fast daylight modeling, even faster than cloud-based tools. Nevertheless, its up-to-date version computes DGPs instead of full DGP for the annual glare simulation. Its daylight simulation has not been integrated with Grasshopper. Therefore, running the annual point-in-time DGP simulation is not practical. In this study, we used a lower rendering quality (ab = 2, ad = 512) for glare simulation using DIVA for Grasshopper to expedite the process. Spot check with a medium rendering quality (ab = 3, ad = 1024) on four representative days (equinox and solstice days, from 9 a.m. to 4 p.m.) shows that the average difference is 7%. The difference for most data points (82.5%) is within 10%, indicating the lower quality rendering is an acceptable setting. However, we do realize this is one major limitation of this study. Future research is required to verify the proposed method using higher quality simulation parameters. Another shortcoming of this study is that the simulation model was not validated, with materials selected from the DIVA library. Experimental studies with a well-calibrated and validated daylight simulation model are needed to address this limitation.

The proposed control strategy highlights human comfort by using glare index as the direct control target. However, like most existing methods, it does not include occupants in the control logic, which could frustrate users as they don't have full control over the shading system [51,52]. As a result, the automated shading system might be overridden by occupants in real-life applications. To improve occupants' acceptance and satisfaction with the automated shading system, future studies should consider including them in the control loop. Additionally, the control algorithm is expected to learn and adapt to occupants' preferences after implementation. For instance, this control goal could be achieved by constantly adjusting the visual comfort setpoint (the threshold for DGP in this study) based on occupants' interactions with the shading devices.

5. Conclusion

To incorporate the concept of visual comfort into the control of automated shading systems, this paper presented a simulation-assisted data-driven method to predict and prevent glare with dynamic shades. Different from existing methods in the literature, the proposed strategy eliminates the use of indoor sensors that can be costly and cause privacy concerns, and intensive real-time daylight simulation that can overload the controller. Specifically, it uses pre-simulated data to develop glare predictive models based on simple MLAs. With solar radiation measurements and the position of the sun as the real-time inputs to feed the predictive models, the control algorithm sets the shading devices to the state that prevents glare and maximizes daylight ingress based on the predicted glare condition at each time step.

The proposed control strategy was verified using climate-based simulation in an existing office building, to control the slat tilt angle of automated internal venetian blinds. Glare predictive models were derived using three common machine learning classification algorithms, including K-nearest neighbor, Support Vector Machine, and Random Forest. Pre-simulated glare data with TMY weather were used to train the models. Simulations with a year's historical weather were used to validate the performance of the control method regarding effectiveness in glare prevention and potential in lighting use reduction as well as view access. It was found that the conventional cut-off angle control only managed to avoid 28.9% of the glare, while the proposed control algorithm successfully prevented 86.5%–96.9% of the glare with better view access. If integrated with lighting control, it could reduce lighting energy use by 80.8% compared to that of default on/off control. Conclusively, it significantly outperformed the cut-off angle control in preventing glare, while exhibiting greater potential in lighting energy savings and providing more view access.

With the elimination of indoor sensors and real-time daylight simulation, as well as the need to collect physically measured data for ML model training, the presented control algorithm can be applied to control window shades on different orientations in open-plan offices. It can also be used in private offices for more customized glare control by accounting for multiple view directions. Moreover, it applies to various shading types, not limited to the venetian blinds in this study. It is promising to act as a feasible glare control solution for real-life applications to provide a comfortable and satisfying indoor luminous environment for the occupants. Experimental studies in the future involving occupants are needed to further verify its validity.

Declaration of competing interest

The authors declare that they have no known competing financial interests or personal relationships that could have appeared to influence the work reported in this paper.

Acknowledgments

This work was supported by the Isabel Sophia Liceaga Discretionary Fund of the School of Architecture at Carnegie Mellon University.

References

[1] M.B.C. Aries, M.P.J. Aarts, J. Van Hoof, Daylight and health: a review of the evidence and consequences for the built environment, Light. Res. Technol. 47 (1) (2015) 6–27.
[2] Y. Al Horr, M. Arif, A. Kaushik, A. Mazroei, M. Katafygiotou, E. Elsarrag, Occupant productivity and office indoor environment quality: a review of the literature, Build Environ. 105 (2016) 369–389, https://doi.org/10.1016/j.buildenv.2016.06.001. Available from.
[3] A. Katsifaraki, Development and Evaluation of a Simulation-Based Adaptive Shading Control for Complex Fenestration Systems, Technische Universitaet Berlin, Germany), 2019.
[4] K.G. Van Den Wymelenberg, Visual Comfort, Discomfort Glare, and Occupant Fenestration Control: Developing a Research Agenda, vol. 10, LEUKOS - J Illum Eng Soc North Am, 2014, pp. 207–221, https://doi.org/10.1080/15502724.2014.939004. Available from.
[5] K. Van Den Wymelenberg, Patterns of occupant interaction with window blinds: a literature review, Energy Build. 51 (2012) 165–176, 2012.
[6] A. Tabadkani, A. Roetzel, H.X. Li, A. Tsangrassoulis, A review of automatic control strategies based on simulations for adaptive facades, Build Environ. 175 (January) (2020), https://doi.org/10.1016/j.buildenv.2020.106801, 106801. Available from.
[7] A.A. Nazzal, New daylight glare evaluation method. Introduction of the monitoring protocol and calculation method, Energy Build. 33 (3) (2001) 257–265.
[8] J. Wienold, J. Christoffersen, Evaluation methods and development of a new glare prediction model for daylight environments with the use of CCD cameras, Energy Build. 38 (7) (2006) 743–757.
[9] J. Wienold, T. Iwata, M. Sarey Khanie, E. Erell, E. Kaftan, R.G. Rodriguez, et al., in: Cross-validation and Robustness of Daylight Glare Metrics [Internet], vol. 51, Lighting Research and Technology, 2019, pp. 983–1013, https://doi.org/10.1177/1477153519826003. Available from.
[10] A. Galatioto, M. Beccali, in: Aspects and Issues of Daylighting Assessment: A Review Study, vol. 66, Renew Sustain Energy Rev [Internet, 2016, pp. 852–860, https://doi.org/10.1016/j.rser.2016.08.018. Available from.
[11] J. Wienold, Dynamic daylight glare evaluation, IBPSA 2009 - Int. Build Perform. Simul. Assoc. (2009) 944–951, 2009.
[12] J. Wienold, Dynamic simulation of blind control strategies for visual comfort and energy balance analysis, IBPSA 2007 - Int. Build. Perform. Simul. Assoc. (2007) 1197–1204, 2007.
[13] C.F. Reinhart, K. Voss, Monitoring manual control of electric lighting and blinds, Light. Res. Technol. 35 (3) (2003) 243–258.
[14] A. Motamed, B. Bueno, L. Deschamps, T.E. Kuhn, J.L. Scartezzini, Self-commissioning glare-based control system for integrated Venetian blind and electric lighting, Build. Environ. 171 (January) (2020).
[15] M. Kim, I. Konstantzos, A. Tzempelikos, Real-time daylight glare control using a low-cost, window-mounted HDRI sensor, Build Environ. 177 (2020), https://doi.org/10.1016/j.buildenv.2020.106912, 106912. Available from.
[16] C. Goovaerts, F. Descamps, V.A. Jacobs, Shading control strategy to avoid visual discomfort by using a low-cost camera: a field study of two cases, Build Environ. 125 (2017) 26–38, https://doi.org/10.1016/j.buildenv.2017.08.030. Available from.
[17] J. Xiong, A. Tzempelikos, Model-based shading and lighting controls considering visual comfort and energy use, Sol. Energy 134 (2016) 416–428, https://doi.org/10.1016/j.solener.2016.04.026. Available from.

[18] Y.C. Chan, A. Tzempelikos, Efficient Venetian blind control strategies considering daylight utilization and glare protection, Sol. Energy 98 (PC) (2013) 241–254.
[19] S. Jain, V. Garg, A Review of Open Loop Control Strategies for Shades, Blinds and Integrated Lighting by Use of Real-Time Daylight Prediction Methods, vol. 135, Build Environ [Internet, 2018, https://doi.org/10.1016/j.buildenv.2018.03.018 (December 2017):352–64. Available from.
[20] A. Nabil, J. Mardaljevic, Useful daylight illuminance: a new paradigm for assessing daylight in buildings, Light. Res. Technol. 37 (1) (2005) 41–59.
[21] J.A. Jakubiec, Validation of simplified visual discomfort calculations, Build. Simul. Optim. Conf. (September) (2018) 11–12.
[22] K. Konis, Predicting Visual Comfort in Side-Lit Open-Plan Core Zones: Results of a Field Study Pairing High Dynamic Range Images with Subjective Responses, vol. 77, Energy Build [Internet, 2014, pp. 67–79, https://doi.org/10.1016/j.enbuild.2014.03.035. Available from.
[23] I. Konstantzos, A. Tzempelikos, Y.C. Chan, Experimental and Simulation Analysis of Daylight Glare Probability Inoffices with Dynamic Window Shades, vol. 87, Build Environ [Internet, 2015, pp. 244–254, https://doi.org/10.1016/j.buildenv.2015.02.007. Available from.
[24] J.Y. Suk, Luminance and Vertical Eye Illuminance Thresholds for Occupants' Visual Comfort in Daylit Office Environments, vol. 148, Build Environ [Internet], 2019, https://doi.org/10.1016/j.buildenv.2018.10.058 (October 2018):107–15. Available from.
[25] S. Torres, V.R.M. Lo Verso, Comparative Analysis of Simplified Daylight Glare Methods and Proposal of a New Method Based on the Cylindrical Illuminance, vol. 78, Energy Procedia [Internet, 2015, pp. 699–704, https://doi.org/10.1016/j.egypro.2015.11.074. Available from.
[26] L. Karlsen, P. Heiselberg, I. Bryn, H. Johra, Verification of simple illuminance based measures for indication of discomfort glare from windows, Build Environ. 92 (2015) 615–626, https://doi.org/10.1016/j.buildenv.2015.05.040. Available from.
[27] J. Mardaljevic, M. Andersen, N. Roy, J. Christoffersen, Daylighting metrics: is there a relation between useful daylight illuminance and daylight glare probability?, in: Proceedings of the Building Simulation and Optimization Conference BSO12, 2012, pp. 189–196.
[28] L. Giovannini, F. Favoino, V.R.M. Lo Verso, A. Pellegrino, V. Serra, A simplified approach for the annual and spatial evaluation of the comfort classes of daylight glare using vertical illuminances, Buildings 8 (12) (2018).
[29] L. Roche, Summertime performance of an automated lighting and blinds control system, Light. Res. Technol. 34 (1) (2002) 11–25.
[30] L. Karlsen, P. Heiselberg, I. Bryn, Occupant satisfaction with two blind control strategies: slats closed and slats in cut-off position, Sol Energy [Internet 115 (2015) 166–179, https://doi.org/10.1016/j.solener.2015.02.031. Available from.
[31] Y. Bian, T. Luo, Investigation of visual comfort metrics from subjective responses in China: a study in offices with daylight, Build Environ. 123 (2017) 661–671, https://doi.org/10.1016/j.buildenv.2017.07.035. Available from.
[32] K. Van Den Wymelenberg, M. Inanici, P. Johnson, The effect of luminance distribution patterns on occupant preference in a daylit office environment, LEUKOS - J. Illum. Eng. Soc. North Am. 7 (2) (2010) 103–122.
[33] J. Wienold, Dynamic daylight glare evaluation, in: Building Simulation, 2009, pp. 944–951, 2009.
[34] M. Ayoub, A Review on Machine Learning Algorithms to Predict Daylighting inside Buildings, vol. 202, Sol Energy [Internet], 2020, https://doi.org/10.1016/j.solener.2020.03.104 (March):249–75. Available from.
[35] S. Mohamed Yacine, Z. Noureddine, B.E.A. Piga, E. Morello, D. Safa, Developing Neural Networks to Investigate Relationships between Lighting Quality and Lighting Glare Indices, vol. 122, Energy Procedia [Internet], 2017, pp. 799–804, https://doi.org/10.1016/j.egypro.2017.07.406. Available from.
[36] I. Chatzikonstantinou, S. Sariyildiz, Approximation of simulation-derived visual comfort indicators in office spaces: a comparative study in machine learning, Archit. Sci. Rev. 59 (4) (2016) 307–322, https://doi.org/10.1080/00038628.2015.1072705. Available from.
[37] S.M. Al-Masrani, K.M. Al-Obaidi, Dynamic Shading Systems: A Review of Design Parameters, Platforms and Evaluation Strategies, vol. 102, Autom Constr [Internet], 2019, https://doi.org/10.1016/j.autcon.2019.01.014 (March):195–216. Available from.
[38] N.S. Altman, An introduction to kernel and nearest-neighbor nonparametric regression, Am. Statistician 46 (3) (1992) 175–185.
[39] L. Saitta, Support-vector networks, Mach. Learn. 297 (1995) 273–297.
[40] L. Breiman, Bagging predictors, Mach. Learn. 24 (2) (1996) 123–140.
[41] R. and A. McNeel, Rhinoceros version 4.0, Serv. Release 8 (2010).
[42] C.F. Reinhart, K. Lagios, J. Niemasz, A. Jakubiec, DIVA for Rhino Version 2.0, 2011.
[43] D. Yang, August, A Correct Validation of the National Solar Radiation Data Base (NSRDB), vol. 97, Renew Sustain Energy Rev [Internet, 2018, pp. 152–155, https://doi.org/10.1016/j.rser.2018.08.023. Available from.
[44] A. Habte, M. Sengupta, A. Lopez, Evaluation of the National Solar Radiation Database (NSRDB Version 2): 1998-2015 [Internet], Nrel/Tp-5D00-67722, 2017. Available from, http://www.osti.gov/servlets/purl/1351859/%0Ahttp://www.nrel.gov/docs/fy17osti/67722.pdf.
[45] M. Sengupta, Y. Xie, A. Lopez, A. Habte, G. Maclaurin, J. Shelby, The National Solar Radiation Data Base (NSRDB) vol. 89, Renew Sustain Energy Rev [Internet], 2018, pp. 51–60, https://doi.org/10.1016/j.rser.2018.03.003. January 2018.
[46] H. Shen, A. Tzempelikos, Daylight-linked Synchronized Shading Operation Using Simplified Model-Based Control, vol. 145, Energy Build [Internet], 2017, https://doi.org/10.1016/j.enbuild.2017.04.021, 200–12. Available from.
[47] Z. Luo, C. Sun, Q. Dong, A Daylight-Linked Shading Strategy for Automated Blinds Based on Model-Based Control and Radial Basis Function (RBF) Optimization, vol. 177, Build Environ [Internet, 2020, https://doi.org/10.1016/j.buildenv.2020.106854 (December 2019):106854. Available from.
[48] A.H. Fakra, H. Boyer, F. Miranville, D. Bigot, A simple evaluation of global and diffuse luminous efficacy for all sky conditions in tropical and humid climate, Renew Energy 36 (1) (2011) 298–306, https://doi.org/10.1016/j.renene.2010.06.042.
[49] A. Motamed, B. Bueno, L. Deschamps, T.E. Kuhn, J.L. Scartezzini, Self-commissioning glare-based control system for integrated Venetian blind and electric lighting, Build. Environ. (2020) 171. December 2019.
[50] S.I. Yun, H.R. Kim, D.Y. Park, J.W. Jeong, Sensor minimization method for integrated daylighting control by a mathematical approach, Energy Build. (2020) 214.
[51] R.J. Cole, Z. Brown, Reconciling human and automated intelligence in the provision of occupant comfort, Intell. Build. Int. 1 (1) (2009) 39–55.
[52] A.D. Galasiu, J.A. Veitch, Occupant preferences and satisfaction with the luminous environment and control systems in daylit offices: a literature review, Energy Build. 38 (7) (2006) 728–742.